pied by resolvase mutants (S10L) that have intact 2-3′ interfaces (including residue Arg^2); thus, the Arg^2 connection (which is made twice at each interface) would only be partially eliminated.

The proposal that the catalytic unit of resolvase consists of a pair of 1,2 dimers has two implications. First, the 1,2 dimer, when bound to site I, must be appreciably distorted from its crystallographic conformation to allow access of the two Ser^{10} residues to the crossover point. We have recently presented other data to support this view (*16*), and Rice and Steitz (*17*) have proposed that a scissorlike movement at the 1,2 interface could bring the two active sites closer together. Second, the two site I–bound 1,2 dimers either have a 222-symmetrical way of interacting with one another that is as yet unrecognized (perhaps mediated by the COOH-terminal 63 residues of resolvase, which are not visible in any crystal forms of the intact protein), or are held by resolvase-resolvase interactions with the rest of the synaptic complex in an equivalent symmetrical manner (*17*) (these two alternatives are, of course, not mutually exclusive). Consideration of the DNA-invertases, a resolvase-related class of site-specific recombinases, exemplified by Hin and Gin suggests that a direct interaction between the two catalytic dimers must occur (*18*). The inversion systems have just one recombinase dimer binding site for each recombination partner, and although these systems use an accessory protein, Fis, pairing of recombination sites can be observed with Hin alone in the absence of Fis (*19*). In addition, Fis-independent mutants of Gin give recombination in the absence of the accessory protein, indicating that the recombinase dimer contains the information necessary for synapsis (*20*).

REFERENCES AND NOTES

1. H. Echols, *J. Biol. Chem.* **265**, 14697 (1990).
2. K. Mizuuchi, *Annu. Rev. Biochem.* **61**, 1011 (1992); N. L. Craig, in *Mobile DNA*, D. E. Berg and M. M. Howe, Eds. (American Society for Microbiology, Washington, D.C., 1989), pp. 211–225.
3. A. Landy, *Annu. Rev. Biochem.* **58**, 913 (1989).
4. G. F. Hatfull and N. D. F. Grindley, in *Genetic Recombination*, R. Kucherlapati and G. R. Smith, Eds. (American Society for Microbiology, Washington, D.C., 1988), pp. 357–396.
5. W. M. Stark, M. R. Boocock, D. J. Sherratt, *Trends Genet.* **5**, 304 (1989).
6. S. A. Wasserman, J. M. Dungan, N. R. Cozzarelli, *Science* **229**, 171 (1985).
7. S. J. Elledge and R. W. Davis, *Genes Dev.* **3**, 185 (1989). Details of the mutagenesis and selection will be published elsewhere. The mutant R172L appeared to be a classical altered specificity mutant; it exhibited repressor activity with the G2T mutant site I but not with the wild-type site (G2) nor with other mutant sites altered at the same position (for example, G2A) or at a different position (for example, T3A). However, the affinity of the R172L mutant resolvase for the G2T mutant site is much lower than the affinity of wild-type resolvase for the wild-type site.
8. V. Rimphanitchayakit and N. D. F. Grindley, *EMBO J.* **9**, 719 (1990).
9. G. F. Hatfull and N. D. F. Grindley, *Proc. Natl. Acad. Sci. U.S.A.* **83**, 5429 (1986).
10. Positive complementation of R172L was also obtained with other catalytically defective mutants, including S10C, R8Q, R68H, and R71H.
11. M. R. Sanderson *et al.*, *Cell* **63**, 1323 (1990).
12. R. E. Hughes, G. F. Hatfull, P. Rice, T. A. Steitz, N. D. F. Grindley, *ibid.*, p. 1331.
13. R. E. Hughes, P. A. Rice, T. A. Steitz, N. D. F. Grindley, *EMBO J.* **12**, 1447 (1993).
14. R. E. Hughes and N. D. F. Grindley, unpublished results.
15. G. F. Hatfull, S. M. Noble, N. D. F. Grindley, *Cell* **49**, 103 (1987).
16. J. M. Mazzarelli, M. R. Ermácora, R. O. Fox, N. D. F. Grindley, *Biochemistry* **32**, 2979 (1993).
17. P. A. Rice and T. A. Steitz, in preparation.
18. R. C. Johnson, *Curr. Biol.* **1**, 404 (1991).
19. K. A. Heichman and R. C. Johnson, *Science* **249**, 511 (1990).
20. A. Klippel, K. Cloppenborg, R. Kahmann, *EMBO J.* **7**, 3983 (1988).
21. Resolution reactions in 20 mM tris-HCl (pH 8.0), 10 mM $MgCl_2$, 100 mM NaCl were initially 10 μl and contained about 0.4 μg of supercoiled substrate DNA and the R172L mutant (1 U ≈ 0.1 μg) as indicated. After incubation for 5 min at 37°C, an additional 10 μl containing the S10L mutant (0.05 μg) or dilution buffer was added, and incubation was continued for a further 20 min. DNAs were then digested with the appropriate restriction enzyme (10 U, 60 min; Bst I for pNG345, Eco RI and Pst I for pNG210). Finally, proteinase K [2 μl of stock solution (10 mg/ml)] was added, and the mixture was incubated for 10 min.
22. DNase I footprinting of resolvase-DNA complexes was as described [N. D. F. Grindley *et al.*, *Cell* **30**, 19 (1982)]. The DNA fragment was a 250-bp Eco RI–Dde I fragment 3′–end labeled at the Eco RI site, proximal to site I^{G2T}.
23. R. R. Reed, *Cell* **25**, 713 (1981).
24. Resolution reactions were set up in two parts. First, a 10-μl reaction (*21*) containing the first mentioned resolvase mutant was incubated for 5 min at 37°C. An additional 10 μl of resolution buffer containing the second mentioned resolvase (or, if only one resolvase is listed, a second portion of the same mutant) was then added, and incubation was continued for a further 30 min before addition of Eco RI (5 U). The amount of each resolvase per 10-μl reaction volume was 0.5 U, to give a total of 1 U of resolvase (or resolvases) per 20-μl final volume.

25. I thank C. Joyce, B. Hughes, J. Mazzarelli, G. Hatfull, and P. Rice for helpful discussions and comments on the manuscript, and K. Tatham for manuscript preparation. Supported by a grant from the NIH. This paper is dedicated to the memory of Hatch Echols.

25 May 1993; accepted 18 August 1993

Calcium Sparks: Elementary Events Underlying Excitation-Contraction Coupling in Heart Muscle

H. Cheng, W. J. Lederer,* M. B. Cannell

Spontaneous local increases in the concentration of intracellular calcium, called "calcium sparks," were detected in quiescent rat heart cells with a laser scanning confocal microscope and the fluorescent calcium indicator fluo-3. Estimates of calcium flux associated with the sparks suggest that calcium sparks result from spontaneous openings of single sarcoplasmic reticulum (SR) calcium-release channels, a finding supported by ryanodine-dependent changes of spark kinetics. At resting intracellular calcium concentrations, these SR calcium-release channels had a low rate of opening (~0.0001 per second). An increase in the calcium content of the SR, however, was associated with a fourfold increase in opening rate and resulted in some sparks triggering propagating waves of increased intracellular calcium concentration. The calcium spark is the consequence of elementary events underlying excitation-contraction coupling and provides an explanation for both spontaneous and triggered changes in the intracellular calcium concentration in the mammalian heart.

Excitation-contraction coupling in heart muscle is triggered by an increase in the concentration of intracellular calcium ($[Ca^{2+}]_i$) due to the sarcolemmal Ca^{2+} current (I_{Ca}), and this increase in $[Ca^{2+}]_i$ is amplified by the SR by a process known as Ca^{2+}-induced Ca^{2+} release (CICR) (*1–3*). CICR also exists in other types of muscle and in many cells with intracellular Ca^{2+} stores (*4, 5*). For the heart, studying CICR in situ has been difficult because of the complex microarchitecture of the muscle cell, which precludes direct examination of intracellular events at the level of single channels. Although the Ca^{2+}-release channel has been studied in reconstitution experiments in planar lipid bilayers and has been identified as the ryanodine receptor (RyR) (*6*), such experiments necessarily preclude examination of the regulation of the release channel in its intracellular environment. Using a laser scanning confocal microscope and the fluorescent Ca^{2+} indi-

H. Cheng, Department of Physiology, University of Maryland School of Medicine, Baltimore, MD 21201.
W. J. Lederer, Department of Physiology and Medical Biotechnology Center, University of Maryland School of Medicine, 660 West Redwood Street, Baltimore, MD 21201.
M. B. Cannell, Department of Physiology, University of Maryland School of Medicine, and Department of Pharmacology and Clinical Pharmacology, St. George's Hospital Medical School, Cranmer Terrace, London SW17 ORE, United Kingdom.

*To whom correspondence should be addressed.

cator fluo-3, we were able to record the activity of SR Ca^{2+}-release channels in their native environment. The results presented here provide an explanation for how the CICR mechanism that is normally activated by I_{Ca} can also give rise to spontaneous Ca^{2+} release and propagating waves of elevated $[Ca^{2+}]_i$ in heart muscle.

A resting heart cell was loaded with the fluorescent Ca^{2+} indicator fluo-3 (*7*) (Fig. 1). The cell was quiescent but could give a large contraction (shortening by 10 to 20%) when stimulated electrically. In a sequence of fluorescence images of the same cell (Fig. 1B), the fluorescence is generally uniform, although there are discrete regions of increased fluorescence ("sparks") that vary in position between images. These sparks reflect spontaneous increases in $[Ca^{2+}]_i$ ("Ca^{2+} sparks") in small regions of the cell at a frequency of about 1.3 s^{-1} in the thin (<1 μm) confocal image section of the cell. The region of increased $[Ca^{2+}]_i$ appeared to be restricted to a circular area with a radius of about 1.5 μm, which is consistent with the spark arising from a point source of Ca^{2+}.

To examine the temporal and spatial properties of the Ca^{2+} spark more closely, we used the confocal microscope in line-scan mode, where a single line across the cell was repeatedly scanned. These scans showed that a Ca^{2+} spark started in a region of the cell about 1 μm across and was confined to a small volume rather than spreading across the cell (Fig. 2A). A Ca^{2+} transient evoked by electrical stimulation rose throughout the cell (Fig. 2B), and it is clear that the duration of the stimulated $[Ca^{2+}]_i$ transient was longer than the Ca^{2+} spark. These data are summarized in Fig. 2C, where the time courses of fluorescence changes associated with a Ca^{2+} spark and stimulated transient are compared. The Ca^{2+} spark and evoked transient both reached a peak in about 10 ms. The spark declined with a half-time of about 20 ms, whereas the decline of the Ca^{2+} transient was slower, with a half-time of about 164 ms. The local increase in $[Ca^{2+}]_i$ associated with the spark was probably removed by the same mechanisms (such as intracellular buffers and Ca^{2+} pumps) that act during the evoked Ca^{2+} transient; the increased rate of decline of the spark can be explained by the buffers being less saturated with Ca^{2+} during the spark. The limited diffusion of the Ca^{2+} spark from the site of initiation may be due to the SR acting as a diffusional barrier, as suggested from experiments in skinned cardiac cells (*1, 2, 8*), which may also help to explain why Ca^{2+} transients (produced by photorelease of caged Ca^{2+}) fail to cause Ca^{2+} release in neighboring regions (*9*).

In principle, a Ca^{2+} spark could arise from Ca^{2+} flux into the cytosol through sarcolemmal Ca^{2+} channels or from Ca^{2+} release by the SR. The former was ruled out by the observation that Ca^{2+} sparks were observed when cells were briefly exposed to bathing medium without Ca^{2+} or to medium supplemented with 0.1 mM cadmium, maneuvers that block entry of extracellular Ca^{2+} through Ca^{2+} channels. The role of the SR Ca^{2+}-release channel was investigated with the specific ligand ryanodine (*10, 11*). Planar lipid bilayer experiments have shown that ryanodine alters SR Ca^{2+}-release channels in a concentration-dependent manner (*11–15*). At low concentrations, ryanodine increases the probability of channel opening, whereas at higher concentrations ryanodine causes long-lasting subconductance states to appear, eventually blocking the channel at micromolar concentrations. These actions of ryanodine on the RyR incorporated into planar lipid bilayers were similar to the effect of ryanodine on Ca^{2+} sparks (Fig. 3). There were no Ca^{2+} sparks in most cells (14 of 15) exposed to concentrations of ryanodine greater than 1 μM (*16*). After 1 to 3 min (*17*) of exposure to intermediate concentrations of ryanodine (100 to 300 nM), the frequency of Ca^{2+} sparks increased from 1.6 ± 0.22 to 3.53 ± 0.75 per line-scan image (mean ± SEM; n = 9). However, some regions showed an even greater increase in spark frequency, and in these regions the spark

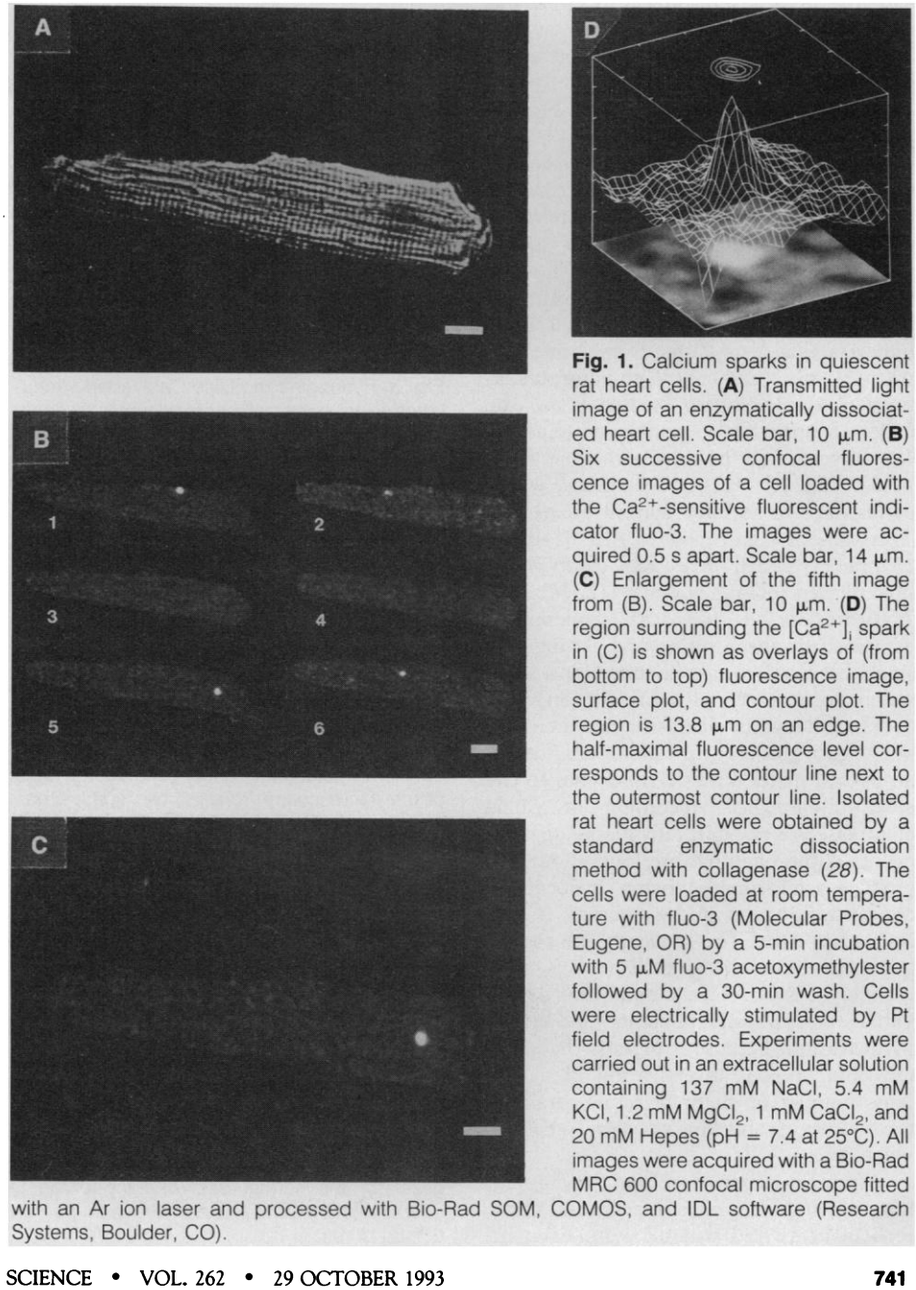

Fig. 1. Calcium sparks in quiescent rat heart cells. (**A**) Transmitted light image of an enzymatically dissociated heart cell. Scale bar, 10 μm. (**B**) Six successive confocal fluorescence images of a cell loaded with the Ca^{2+}-sensitive fluorescent indicator fluo-3. The images were acquired 0.5 s apart. Scale bar, 14 μm. (**C**) Enlargement of the fifth image from (B). Scale bar, 10 μm. (**D**) The region surrounding the $[Ca^{2+}]_i$ spark in (C) is shown as overlays of (from bottom to top) fluorescence image, surface plot, and contour plot. The region is 13.8 μm on an edge. The half-maximal fluorescence level corresponds to the contour line next to the outermost contour line. Isolated rat heart cells were obtained by a standard enzymatic dissociation method with collagenase (*28*). The cells were loaded at room temperature with fluo-3 (Molecular Probes, Eugene, OR) by a 5-min incubation with 5 μM fluo-3 acetoxymethylester followed by a 30-min wash. Cells were electrically stimulated by Pt field electrodes. Experiments were carried out in an extracellular solution containing 137 mM NaCl, 5.4 mM KCl, 1.2 mM $MgCl_2$, 1 mM $CaCl_2$, and 20 mM Hepes (pH = 7.4 at 25°C). All images were acquired with a Bio-Rad MRC 600 confocal microscope fitted with an Ar ion laser and processed with Bio-Rad SOM, COMOS, and IDL software (Research Systems, Boulder, CO).

amplitude could be described by a single Gaussian distribution. The sparks from these regions also showed a normal rate of decay [half-time of decay ($t_{1/2}$) = 22.3 ± 1.12 ms, mean ± SEM; n = 40], which suggests that ryanodine had increased only the probability of spark occurrence in these regions. A second type of behavior induced by ryanodine was the appearance of lower amplitude sparks of long duration (Fig. 3), which resembled the ryanodine-induced, long-lasting subconductance state observed in single-channel records. Despite repeated long openings of the RyR (Fig. 3B, trace 1-1), there was little reduction in the amplitude of the spark during the openings (Fig. 3B, traces 1-1 and 3-3), which suggests that there is considerable local Ca^{2+} recycling. This finding is also consistent with the limited spreading of Ca^{2+} sparks seen in line-scan images (Fig. 2).

The flux of calcium (J) associated with a spark will be

$$J = B \cdot \Delta[Ca^{2+}]_i \cdot V \cdot T^{-1}$$

where B is the buffering power of the cell for Ca^{2+} [released Ca^{2+} (μM)/increase in $[Ca^{2+}]_i$ (μM)], $\Delta[Ca^{2+}]_i$ is the concentration change during the spark, V is the volume occupied by the spark, and T is the time taken for the rise of $[Ca^{2+}]_i$. Examination of data like that shown in Figs. 1 and 2 indicates that $V \approx 10$ fl, $T \approx 10$ ms, and $\Delta[Ca^{2+}]_i \approx 0.2$ μM (*18*). Computer simulations of Ca^{2+} binding by fluo-3 and the major intrinsic Ca^{2+} binding proteins (*2*, *19*) suggests that in these experiments, $B \approx 100$. Thus, $J \approx 2 \times 10^{-17}$ mol/s, which corresponds to an ionic current of ~4 pA. This value is comparable to that of single-channel currents from the RyR (*6*) in planar lipid bilayers [~3 pA at 0 mV (*12*, *14*, *20*)]. Thus, we conclude that a Ca^{2+} spark may be explained by the opening and closing of a single SR Ca^{2+}-release channel (or a small number of channels acting in concert).

These data provide in situ measurements of the gating of an intracellular channel by an optical method that is analogous to the electrophysiological recording of single channels. We can faithfully record opening events if the openings are long enough to produce a measurable change in local ion concentration and if the opening is well isolated in time. This is clearly the case in quiescent living heart cells with a large number of RyRs. This method has an advantage over traditional planar lipid bilayer investigations because it permits the virtually simultaneous investigation of a very large number of channels while retaining the sensitivity and kinetics to record individual events.

Although information from the cloning, imaging, and anatomical localization of the RyR in heart and skeletal muscle has increased rapidly (*21*), functional investigations have been impeded because the RyR is located in the intracellular compartment. Of the approximately 10^6 ryanodine receptors per rat heart cell (*22*), approximately 10^5 can be surveyed simultaneously by the confocal imaging method described here, which views approximately 10% of the cell volume. The measured opening rate (about 0.0001 s^{-1}) suggests that about 100 sparks per second occur in the whole cell at rest (*22*), each leading to a ~170 nM elevation of $[Ca^{2+}]_i$ (*18*) above the resting level of 100 nM with a half-time of decay of ~25 ms ($t_{1/2}$ = 24.5 ms ± 1.86, mean ± SEM; n = 20) in regions ~2 μm across. When Ca^{2+} "overload" (that is, increasing SR Ca^{2+} content above normal) was produced by increasing the extracellular Ca^{2+} concentration to 10 mM, the opening rate was

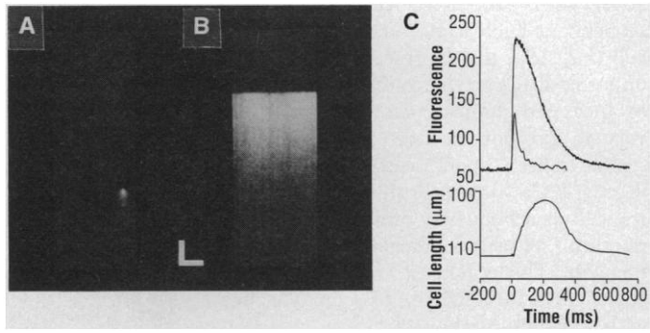

Fig. 2. Line-scan images of heart cells, showing the kinetics of $[Ca^{2+}]_i$ transients in rat heart cells. (**A**) A quiescent heart cell loaded with fluo-3 viewed by repetitive line scans in a fixed location reveals a localized elevation of intracellular Ca^{2+} at high temporal resolution. Each line scan is acquired in 2 ms. The first line is displayed at the top of the image, and successive lines are added below. Thus, time runs from the top to the bottom of the image (scale bar, 100 ms) and distance across the scanned region from left to right (scale bar, 10 μm). (**B**) The same cell in (A) was field-stimulated (2-ms square wave stimulation at 2× threshold) 280 ms after the scan was initiated. A significant elevation of fluorescence arose simultaneously across the cell. (**C**) Comparison of the fluorescence signal associated with the Ca^{2+} spark with the signal from the stimulated $[Ca^{2+}]_i$ transient. The cell contraction activated by the stimulation is shown in the bottom panel.

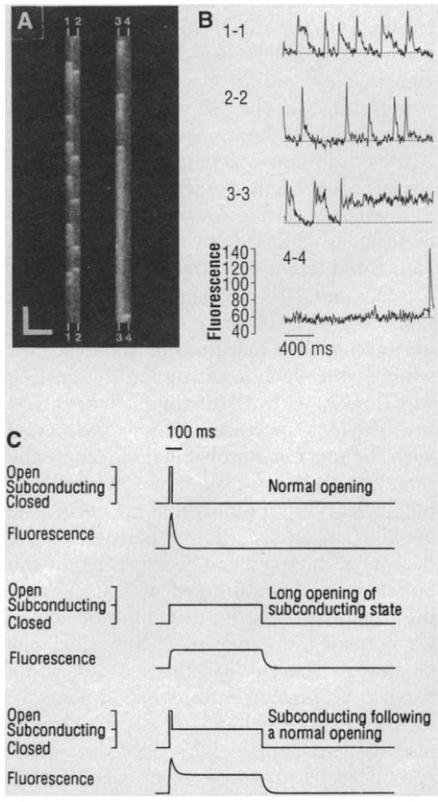

Fig. 3. Ryanodine modifies Ca^{2+} sparks measured in rat heart cells from line-scan images. (**A**) Two line-scan images of a small region of a heart cell taken in sequence. In each of the images, there are two sparking areas. The images were obtained after the cell was exposed to 100 nM ryanodine. Lanes 1 and 3 mark the same site in successive images, and lanes 2 and 4 mark another sparking site (vertical scale bar, 200 ms; horizontal scale bar, 10 μm). Note that the region depicted in lanes 1 and 3 goes from frequent sparking (lane 1) to a continuous signal (lane 3), whereas the neighboring region demonstrates frequent sparking of normal half-time ($t_{1/2}$ = 22.8 ms ± 1.35 ms, mean ± SEM; n = 6) (lane 2) that becomes transiently quiet (lane 4). (**B**) Time-course plots of the fluorescence from the two spark areas identified in (A). The horizontal lines show the base line fluorescence level. Trace 1-1 shows long-duration sparks, whereas trace 2-2 shows an increased number of sparking events of normal duration. Note that the sparking regions appear to behave independently despite their proximity to each other. Trace 3-3 shows an example of a long-duration spark of reduced amplitude that was stable for more than 1 s. Trace 4-4 shows a spark of normal duration, despite the fact that this region was only 2 μm away from the region that gave trace 3-3. (**C**) A schematic diagram showing the hypothesized relation between channel opening and fluorescence intensity at a sparking site. Examples are given for the normal brief opening of an SR Ca^{2+}-release channel, the long opening of a subconducting state of the channel, and a normal opening followed by a subconducting opening of long duration.

increased around fourfold (402 ± 83%, mean ± SEM, $n = 9$) (Fig. 4, A and B).

It is notable that in these conditions, propagating waves of elevated $[Ca^{2+}]_i$ regularly appear, although there was only a modest increase in the rate of spark occurrence. In a line-scan image of the site of initiation of a wave (Fig. 4C), the wave appeared as an inverted "V" because of the propagation of the wave from the site of initiation. There were several sparks in this region before the wave started, and at the point of initiation a "macrospark" occurred, which reached a peak of about 500 nM. Because the normal spark has a peak $[Ca^{2+}]_i$ between 200 and 300 nM, the larger initiating spark may be the result of a summation of several closely spaced individual sparks. Of 18 propagating waves whose sites of initiation have been imaged with line-scan images, 10 have sparks or macrosparks at that site, which suggests that these sparks act as initiating triggers. The transition from nonpropagating sparks to waves cannot be explained simply by the increase in spark frequency, as the elevation of spark frequency with ryanodine does not produce propagating waves of increased $[Ca^{2+}]_i$. Instead, the sensitivity of the SR Ca^{2+}-release channel for activation by cytosolic Ca^{2+} may increase as a consequence of the greater amount of Ca^{2+} stored in the SR in these conditions. This explanation is consistent with the observation that although stimulated, cell-wide Ca^{2+} transients require local Ca^{2+} currents to activate SR Ca^{2+} release, local Ca^{2+} currents are not needed to support the propagating waves of elevated $[Ca^{2+}]_i$ during Ca^{2+} overload (*9, 23, 24*). Thus, the process of CICR appears to be more readily triggered during Ca^{2+} overload. Just as a high concentration of ryanodine blocks the SR Ca^{2+}-release channel in bilayers and the depolarization-activated SR Ca^{2+} release in heart muscle, a high concentration of ryanodine blocks the propagating waves of elevated $[Ca^{2+}]_i$ during Ca^{2+} overload (*24, 25*).

The cardiac RyR is one member of a superfamily of membrane proteins expressed in a variety of tissues (*4*). We have examined the cardiac RyR in its native environment under normal physiological conditions, during Ca^{2+} overload, and after pharmacological modification. The opening rate of the cardiac RyR under normal conditions is extremely low and propagating CICR does not occur. This suggests that the amplification of a spark by CICR is insufficient to cause regenerative release under normal conditions. Thus, the efficient coupling of the Ca^{2+} current to CICR may depend on the close anatomical proximity of the sarcolemmal Ca^{2+} channels to the RyR in the proposed "fuzzy space" (*26*). The initiation of propagating waves of CICR by spontaneous Ca^{2+} sparks suggests that CICR becomes more sensitive to an increase in $[Ca^{2+}]_i$ during Ca^{2+} overload. With the methods described here, it should be possible to examine time- and second messenger–dependent modulation of the sensitivity of CICR in a variety of tissues.

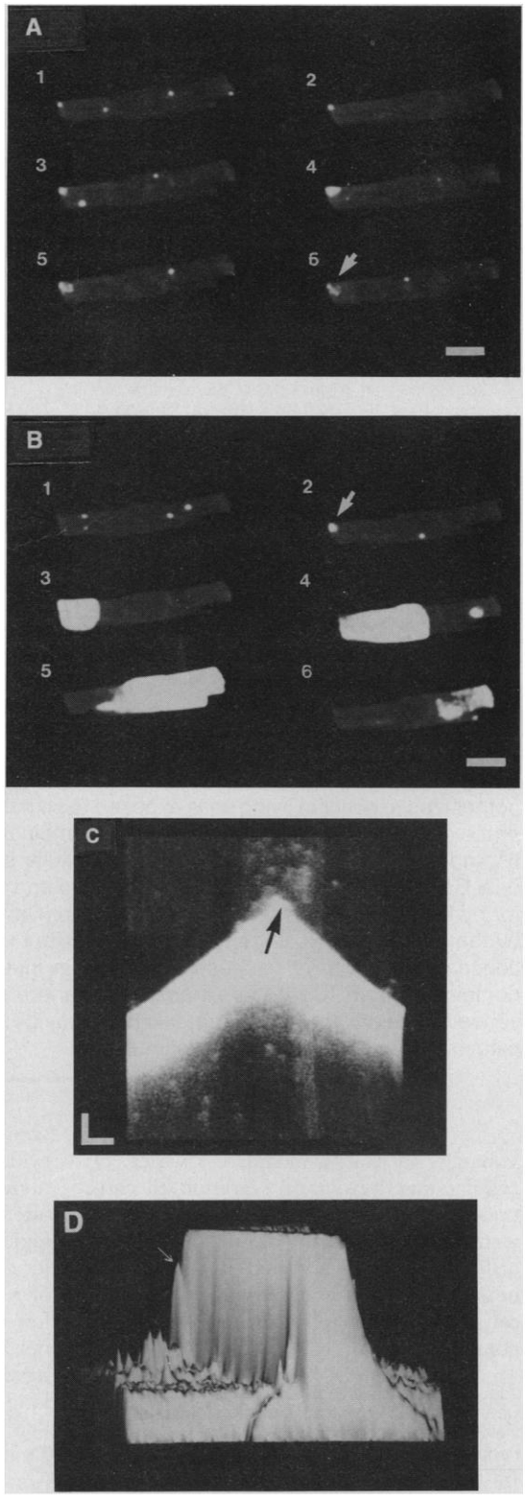

Fig. 4. Calcium overload increases the frequency of Ca^{2+} sparks and propagating waves of increased intracellular Ca^{2+}. (**A**) Calcium sparks in a fluo-3–loaded cell subjected to Ca^{2+} overload. Calcium overload was produced by increasing Ca^{2+} in the bathing solution to 10 mM. Sequential images were obtained every 0.5 s. Sparks are numerous in these images, and at the left of the cell a spark appears to recruit more sparks before decaying (arrow). Scale bar, 20 μm. (**B**) Sequence of images of the same cell as shown in (A) taken 4 min later. These images show the development of a spreading wave of increased intracellular Ca^{2+} from the region (arrow) that recruited sparks in (A). (**C**) Line-scan image obtained in a Ca^{2+}-overloaded cell reveals the origin of a propagating wave of elevated Ca^{2+}. Calcium sparks are plentiful in this line-scan image before and after the propagating wave, and at the site of initiation of the wave (the apex of the wave front) there were several sparks, one of which activates the spreading wave [marked with an arrow here and in (D)]. The wave of elevated intracellular Ca^{2+} propagated at a speed of 70 μm/s. (Scale bar, 10 μm horizontal, 200 ms vertical.) (**D**) A shaded surface plot of the line scan shown in (C). Time is plotted from left to right, and the viewpoint is from the upper right corner of (C). Height is a measure of fluorescence intensity. The surface plot reveals three features. (i) The triggering event occurs at the apex of the inverted "V" and appears to be a macrospark, identified by an arrow. Macrosparks are the result of a single spark recruiting additional sparks as judged by the broader fluorescence area and the greater fluorescence intensity. (ii) Numerous Ca^{2+} sparks appear in front of the propagating wave of elevated $[Ca^{2+}]_i$ (that is, before it was activated). (iii) The small sparks have a peak $[Ca^{2+}]_i$ of about 200 nM, the macrospark has a peak of 533 nM, and the truncation of the propagating wave occurs at 900 nM (because of the limited dynamic range of the confocal light detector subsystem).

REFERENCES AND NOTES

1. A. Fabiato, *J. Gen. Physiol.* **85**, 189 (1985).
2. _____, *ibid.*, p. 291.
3. _____, *Am. J. Physiol.* **245**, C1 (1983); _____ and F. Fabiato, *J. Physiol.* (*London*) **249**, 469 (1975).
4. V. Sorrentino and V. Volpe, *Trends Pharmacol. Sci.* **14**, 98 (1993).
5. P. S. McPherson *et al.*, *Neuron* **7**, 17 (1991); P.

Sah, K. Francis, E. M. McLachlan, P. Junankar, *Neuroscience* **54**, 157 (1993); A. H. Cornell-Bell, S. M. Finkbeiner, M. S. Cooper, S. J. Smith, *Science* **247**, 470 (1990); J. D. Lechleiter and D. E. Clapham, *Cell* **69**, 283 (1992); P. Camacho and J. D. Lechleiter, *Science* **260**, 226 (1993).
6. M. Fill and R. Coronado, *Trends Neurosci.* **11**, 453 (1988).
7. A. Minta, J. P. Y. Kao, R. Y. Tsien, *J. Biol. Chem.* **264**, 8171 (1989).
8. A. Fabiato, *J. Gen. Physiol.* **85**, 247 (1985).
9. S. C. ONeill, J. G. Mill, D. A. Eisner, *Am. J. Physiol.* **258**, C1165 (1990).
10. J. L. Sutko, K. Ito, J. L. Kenyon, *Fed. Proc.* **44**, 2984 (1985); G. Meissner, *Adv. Exp. Med. Biol.* **311**, 277 (1992).
11. G. Meissner and A. el Hashem, *Mol. Cell Biochem.* **114**, 119 (1992).
12. E. Rousseau and G. Meissner, *Am. J. Physiol.* **256**, H328 (1989).
13. E. Buck, I. Zimanyi, J. J. Abramson, I. N. Pessah, *J. Biol. Chem.* **267**, 23560 (1992); I. N. Pessah and I. Zimanyi, *Mol. Pharmacol.* **39**, 679 (1991); F. A. Lai, M. Misra, L. Xu, H. A. Smith, G. Meissner, *J. Biol. Chem.* **264**, 16776 (1989).
14. E. Rousseau, J. S. Smith, G. Meissner, *Am. J. Physiol.* **253**, C364 (1987).
15. G. Meissner, *J. Biol. Chem.* **261**, 6300 (1986).
16. H. Cheng, W. J. Lederer, M. B. Cannell, unpublished data.
17. Both the kinetics and the steady-state–equilibrium conditions of ryanodine binding are dependent on the concentration of ryanodine used. Equilibrium binding of ryanodine at very low concentrations takes several hours and is consequently difficult to achieve in experiments with single heart cells. We have taken advantage of the more rapid onset of low-dose effects when intermediate concentrations of ryanodine (100 nM) are applied to observe behavior normally associated with lower concentrations of ryanodine. The ryanodine off-rate is sufficiently low so that the binding is essentially irreversible (over the time scale of these experiments).
18. At a single wavelength
$$[Ca^{2+}] = K(F - F_{min})/(F_{max} - F)$$
where K is the dissociation constant for the indicator, F_{min} is the fluorescence in the absence of Ca^{2+}, and F_{max} is the fluorescence in the presence of saturating Ca^{2+}. For fluo-3, $F_{min} \approx 0$, so that only estimates of F_{max} and K are required to calibrate the data. F_{max} can be estimated from the rest (control) level of fluorescence because
$$F_{max} = F_{rest}(K/[Ca^{2+}]_{rest} + 1)$$
if there is no change in dye concentration or path length (a condition made more likely with the use of a confocal microscope with negligible photobleaching during the scan). Thus, dividing images by a control image will give a pseudo-ratio image in which
$$[Ca^{2+}] = KR/[(K/[Ca^{2+}]_{rest} + 1) - R]$$
where R is the fluorescence ratio and $[Ca^{2+}]_{rest}$ is the known $[Ca^{2+}]$ in the control image. Assuming K is 400 nM and the resting $[Ca^{2+}]_i$ is 100 nM, we estimate the peak $[Ca^{2+}]$ of a typical Ca^{2+} spark to be about 270 nM and a typical electrically evoked transient to be about 1.46 μM with this method. This estimate of the peak of the evoked transient is consistent with earlier estimates ratiometric dyes [M. B. Cannell, J. R. Berlin, W. J. Lederer, *Science* **238**, 1419 (1987)].
19. W. G. Wier and D. T. Yue, *J. Physiol.* (*London*) **376**, 507 (1986); K. R. Sipido and W. G. Wier, *ibid.* **435**, 605 (1991).
20. A. Tinker, A. R. G. Lindsay, A. J. Williams, *J. Gen. Physiol.* **100**, 495 (1992).
21. B. A. Block, T. Imagawa, K. P. Campbell, C. Franzini-Armstrong, *J. Cell Biol.* **107**, 2587 (1988); F. Zorzato *et al.*, *J. Biol. Chem.* **265**, 2244 (1990); A. R. Marks *et al.*, *Proc. Natl. Acad. Sci. U.S.A.* **86**, 8683 (1989); M. Inui, A. Saito, S. Fleischer, *J. Biol. Chem.* **262**, 15637 (1988); *ibid.* **263**, 10843 (1988).
22. We calculated the opening rate of the SR Ca^{2+}-release channel as follows: The number of RyRs per adult rat heart cell is estimated to be about 1.0×10^6 per cell on the basis of data given by Bers and co-workers (*27*). This estimate arises from the number of dihydropyridine receptors (DHPRs) per surface area (14.8 per square micrometer), the surface-to-volume ratio (0.6 μm^2 per cubic micrometer), the volume of our cells ($\approx 2.0 \times 10^4$ μm^3), and the number of RyRs per DHPR (around seven) (*27*). (Surface area includes the transverse-tubular membranes.) If a cardiac myocyte contains g ryanodine receptors and if we survey a fraction m of the entire cell with a raster scan once over a period of n seconds observing p sparks and the spark is observable for q seconds, then the opening rate r is given by
$$r = p/(gmnq/n) = p/(gmq)$$
assuming that a spark corresponds to a single-channel opening (where the fraction q/n compensates for missed events). A similar approach can be used for a line-scan image, where m should be calculated with respect to the geometry scanned. Taking both lens resolution and the spatial spreading of sparks into account, each scan surveys a volume V_s of approximately 2 μm by 2 μm multiplied by the length of the line scanned. Thus, $m = V_s/V_{cell}$. For a typical heart cell with dimensions of 10 by 20 by 100 μm, V_{cell} is 2×10^4 μm^3. Because the lifetime of a spark is much longer than the time taken to scan a line (2 to 4 ms), compensation for missed events is not needed. Hence, $r = p/(gmn)$. Here, the estimate of r was $1.10 \times 10^{-4} \pm 0.22 \times 10^{-4}$ s^{-1} (mean ± SEM; $n = 13$) based on the line-scan image data. Estimates of r by whole-cell imaging were similar [$r = 1.23 \times 10^{-4} \pm 0.17 \times 10^{-4}$ (mean ± SEM; $n = 18$)]. A change in $[Ca^{2+}]_i$ of >50 nM is needed to recognize a spark, and openings less than about 2 ms would probably be missed.
23. M. Valdeolmillos, S. C. ONeill, G. L. Smith, D. A. Eisner, *Pfluegers Arch.* **413**, 676 (1989); J. R. Berlin, M. B. Cannell, W. J. Lederer, *Circ. Res.* **65**, 115 (1989); *Am. J. Physiol.* **253**, H1540 (1987); T. Takamatsu and W. G. Wier, *Cell Calcium* **11**, 111 (1990); R. S. Kass, W. J. Lederer, R. W. Tsien, R. Weingart, *J. Physiol.* (*London*) **281**, 187 (1978); P. Arlock and B. G. Katzung, *ibid.* **360**, 105 (1985); P. Lipp and L. Pott, *ibid.* **397**, 601 (1988).
24. W. G. Wier, M. B. Cannell, J. R. Berlin, E. Marban, W. J. Lederer, *Science* **235**, 325 (1987).
25. M. B. Cannell, R. D. Vaughan-Jones, W. D. Lederer, *Fed. Proc.* **44**, 2964 (1985); E. Marban and W. G. Wier, *Circ. Res.* **56**, 133 (1985); W. G. Wier, D. T. Yue, E. Marban, *Fed. Proc.* **44**, 2989 (1985).
26. J. S. K. Sham, L. Cleemann, M. Morad, *Science* **255**, 850 (1992); J. R. Hume, P. C. Levesque, N. Leblanc, *ibid.* **251**, 1370 (1991); W. J. Lederer, E. Niggli, R. W. Hadley, *ibid.*, p. 1371; P. C. Levesque, N. Leblanc, J. R. Hume, *Ann. N.Y. Acad. Sci.* **639**, 386 (1991); N. Leblanc and J. R. Hume, *Science* **248**, 372 (1990); W. J. Lederer, E. Niggli, R. W. Hadley, *ibid.*, p. 283.
27. W. Y. W. Lew, L. V. Hryshko, D. M. Bers, *Circ. Res.* **69**, 1139 (1991); D. M. Bers and V. M. Stiffel, *Am. J. Physiol. Cell Physiol.* **264**, 1587 (1993).
28. R. Mitra and M. Morad, *Am. J. Physiol.* **249**, H1056 (1985).
29. Supported by NIH, the University of Maryland Graduate Assistantship program, and the British Heart Foundation. We thank R. Hadley, M. Kirby, T. Rogers, R. Bloch, and H. Valdivia for valuable discussion of the material presented here and for comments on the manuscript.

30 July 1993; accepted 1 October 1993

Microdomains with High Ca^{2+} Close to IP_3-Sensitive Channels That Are Sensed by Neighboring Mitochondria

Rosario Rizzuto,* Marisa Brini, Marta Murgia, Tullio Pozzan

Microdomains of high intracellular calcium ion concentration, $[Ca^{2+}]_i$, have been hypothesized to occur in living cells exposed to stimuli that generate inositol 1,4,5-trisphosphate (IP_3). Mitochondrially targeted recombinant aequorin was used to show that IP_3-induced Ca^{2+} mobilization from intracellular stores caused increases of mitochondrial Ca^{2+} concentration, $[Ca^{2+}]_m$, the speed and amplitude of which are not accounted for by the relatively small increases in mean $[Ca^{2+}]_i$. A similar response was obtained by the addition of IP_3 to permeabilized cells but not by perfusion of cells with Ca^{2+} at concentrations similar to those measured in intact cells. It is concluded that in vivo, domains of high $[Ca^{2+}]_i$ are transiently generated close to IP_3-gated channels and sensed by nearby mitochondria; this may provide an efficient mechanism for optimizing mitochondrial activity upon cell stimulation.

Changes in $[Ca^{2+}]_i$ modulate a variety of cellular functions, from secretion to contraction, enzyme activation, and cell cycle regulation (*1*). Imaging of $[Ca^{2+}]_i$ in living cells (*2*, *3*) has revealed not only the heterogeneity of responses within the same cell population but also complex spatiotemporal patterns in the changes of $[Ca^{2+}]_i$ evoked by receptor stimulation (*1*). Even in nonexcitable cells, increases in $[Ca^{2+}]_i$ are often composed of series of asynchronous rapid oscillations or waves (*4*) or of large local increases, often far away from the site of receptor activation (*5*). However, with few exceptions (Ca^{2+}-activated ion channels) (*6*), it is still unknown whether cells have systems capable of sensing and translating large but localized increases in $[Ca^{2+}]_i$ into metabolic responses. Obvious candidates for detecting regional changes of $[Ca^{2+}]_i$ would be enzymes or organelles that

Department of Biomedical Sciences, CNR Center for the Study of Mitochondrial Physiology, University of Padova, Via Trieste 75, 35121 Padova, Italy.

*To whom correspondence should be addressed.